J Mater Sci (2010) 45:1366–1370
DOI 10.1007/s10853-009-4094-3

The effects of temperature on the molecular orientation of zinc phthalocyanine films

Luciana Gaffo · Márcia R. Cordeiro · Adonilson R. Freitas · Wania C. Moreira · Emerson M. Girotto · Valtencir Zucolotto

Received: 30 June 2009 / Accepted: 28 November 2009 / Published online: 19 December 2009

Abstract Phthalocyanine compounds have been widely investigated as candidate materials for technological applications, which is mainly due to their thermal stability and possibility of processing in the form of thin films. In most applications, the controlled growth of thin films with high crystalline quality is essential. In this study, zinc phthalocyanine (ZnPc) thin films were prepared by evaporation on glass and Au-coated glass substrates with subsequent annealing at different temperatures in ambient atmosphere. The morphological and structural features of 80 nm thick zinc phthalocyanine films were investigated, evidencing an $\alpha \rightarrow \beta$ phase transformation after annealing the films at 200 °C, as indicated by UV–Vis spectroscopy and FTIR analyses. A better uniformity of the annealed films was also evidenced via AFM analysis, which may be of importance for applications where film homogeneity and excellent optical quality are required.

Introduction

Due to their thermal and chemical stability, phthalocyanines have found several applications in the chemical industry as pigments, catalysts, and electrochemical reduction of oxygen, to name a few [1–5]. Some types of phthalocyanines, for example, can resist at temperatures close to 900 °C in vacuum, or ca. 500 °C in an ambient atmosphere [6]. Other applications have been explored, which include molecular electronics [7], non-linear optics [8], liquid crystals [9], gas sensors [1, 10, 11], photovoltaic cells [12], and photodynamic therapy [13, 14]. Alarjah et al. have reported the carbon monoxide gas sensitivity using substituted iron(II) phthalocyanine [2, 3]. Most of the interesting properties of phthalocyanines come from the possibility of the high control over ordering and molecular packing in the solid state [1]. Phthalocyanine thin films may be prepared by several techniques like vacuum evaporation and Langmuir–Blodgett [15–17]. For many applications, the controlled growth of thin films with high crystalline quality is essential [18, 19]. In this case, parameters such as substrate surface and deposition temperature are crucial for fabrication of high-quality films.

There has been a special interest in the structural variations of phthalocyanine thin films [20]. For example, X-ray diffraction and optical absorption have been used to analyze the changes in the crystalline phases of CuPc thin films as a function of temperature [21]. Using metal-free phthalocyanines, Heutz et al. [18, 22] investigated the influence of temperature on the formation of alpha (α) and beta (β) crystalline phases. Two sets of evaporated films were investigated: (i) films deposited at room temperature and subjected to further thermal treatment at high temperatures and (ii) films evaporated over heated substrates. In both cases, an $\alpha \rightarrow \beta$ phase transformation was observed for temperatures higher than 300 °C. For zinc phthalocyanine (ZnPc) evaporated films, in particular, the effects of temperature on the phase transition have been investigated mainly using X-ray diffractometry [23, 24].

L. Gaffo (✉) · A. R. Freitas · E. M. Girotto
Departamento de Química, Universidade Estadual de Maringá, 87020-900 Maringá, PR, Brazil
e-mail: lugaffo@yahoo.com.br

M. R. Cordeiro · W. C. Moreira
Departamento de Química, Universidade Federal de São Carlos, 13565-905 São Carlos, SP, Brazil

V. Zucolotto
Instituto de Física de São Carlos, Universidade de São Paulo, 13560-970 São Carlos, SP, Brazil

In the present paper, we investigate the effect of temperature on the molecular organization of ZnPc upon performing a detailed vibrational characterization of the evaporated films, using reflection absorption infrared spectroscopy (RAIRS) and Raman spectroscopy. Film morphology was also analyzed by ultraviolet–visible absorption (UV–VIS) and Atomic Force Microscopy (AFM).

Experimental

ZnPc was synthesized following the Kirin route [25] using a mixture of zinc acetate dihydrate and phthalonitrile (1:4 mole ratio). The reagents were heated in a glass tube at 300 °C for 3 h. The resulting blue solid powder was washed with water, ethanol, and methanol and extracted in a Soxhlet apparatus with acetone. ZnPc was dried at 120 °C for 2 h. The compound was characterized by UV–VIS (DMF/$CHCl_3$ solution) and Fourier Transform Infrared (FTIR) spectroscopy using KBr pellets. Elemental analysis gave the following results: C, 63.4; H, 3.0; N, 17.5%, which are consistent with the calculated values for ZnPc.$2H_2O$: C, 64.5; H, 3.0; N, 18.8% [26].

ZnPc evaporated films were obtained on pre-cleaned transparent borosilicate slides (glass), zinc selenide (ZnSe), mica and Au-coated glass substrates. ZnPc was evaporated using a BOC Edwards model 306 vacuum system at room temperature. The nominal background pressure was 10^{-6} Torr.

ZnPc was deposited as a thin film with a thickness of 80 nm, as measured by a quartz crystal oscillator coupled to the evaporation system. After deposition, films deposited on glass, Au-coated glass, and mica substrates were treated at temperatures between 50 and 200 °C for 3 h in ambient atmosphere.

UV–VIS spectra of films evaporated on glass were obtained in a Hitachi U-2001 UV–VIS spectrophotometer. FTIR transmission (KBr pellets and evaporated films deposited onto zinc selenide) and reflection–absorption infrared (RAIRS) (films evaporated on Au-coated glass substrates) were recorded using a Thermo Nicolet Nexus 470 FTIR spectrophotometer with 164 scans and spectral resolution of 4 cm^{-1}. Raman spectra of ZnPc films evaporated on glass were obtained with a Renishaw Research Raman Microscope system RM 2000 equipped with a computer controlled 3-axis encoded (XYZ) motorized stage (minimum step of 0.1 μm) and a Leica microscope (DMLM series). The spectra were recorded with the 514 nm laser line using 50% laser power, 10 s collecting time, and three accumulations.

ZnPc evaporated films on glass were analyzed by X-ray diffraction in a Rigaku RU-200 B diffractometer, 2θ varying between 1° and 40°.

AFM measurements were obtained in an Atomic Force Microscope from Shimadzu, model CTM-9500 J3 in tapping mode for ZnPc films deposited on mica The images were obtained before and after heating the film at 200 °C for 3 h.

Results and discussion

The UV–VIS spectra of ZnPc evaporated films before and after annealing for 3 h are shown in Fig. 1. The UV–VIS spectra of ZnPc cast and LB films deposited on glass display the Q band at 687 nm with the satellite band at 627 nm, which is red shifted in comparison to the spectrum in DMF/$CHCl_3$ solution [26] (Q band at 672 nm with a satellite at 606 nm), which is consistent with J aggregates formation [27]. For evaporated films, two absorption maxima were observed at 633 and 695 nm. A small decrease in the absorbance intensity was the only change observed after annealing the film at 100 °C, whereas after annealing at 150 °C, a significant decrease in the absorbance intensity was observed. The position and the intensity of the bands changed drastically after annealing at 200 °C, with two absorption maxima, at 650 and 752 nm, and a shoulder at 820 nm. Furthermore, the relative intensity of the band at 650 nm decreased, which is in concordance with the formation of ZnPc β phase [23].

Vibrational spectroscopy may be used to study the molecular organization of thin films. The relative intensity of vibrational bands in transmission and reflection geometry may provide information on the film dipole moment orientation [28]. Experimental reflection infrared and Raman techniques are based on a theory developed by Greenler [29], who showed the advantage of using light at high incidence angle to investigate molecules absorbed on metal surfaces. The relative intensity of the bands, related to the in-plane and out-of-plane C–H deformation, may

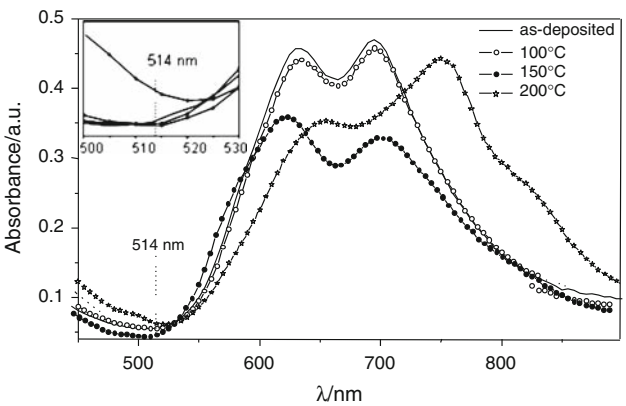

Fig. 1 Electronic absorption spectra of ZnPc evaporated films before and after annealing at 100, 150, and 200 °C

indicate if molecules adopt a preferential orientation on the substrates. If the macrocycle ring is in a face-on organization, in-plane vibrations exhibit maxima relative intensities in transmission spectra and minima intensities in reflectance spectra [30]. The opposite is observed if the macrocycle plane is perpendicular to the substrate surface. FTIR spectra of ZnPc KBr pellet and evaporated films in the transmission and reflectance geometries are displayed in Fig. 2. The bands observed, their assignments and relative intensities (given in parentheses), are shown in Table 1. The KBr pellet spectrum is characterized by out-of-plane C–H mode (726 cm^{-1}), in-plane C–H bend modes (1088, 1118, and 1291 cm^{-1}) and in-plane pyrrole stretching (1332 cm^{-1}). The ZnPc film transmission geometry spectrum is dominated by weak in-plane mode intensities. The most intense band was the out-of-plane mode at 723 cm^{-1}. In-plane mode bands (752, 1092, 1117, and 1333 cm^{-1}) showed reduced intensities. The reflectance spectrum showed opposite features with in-plane mode bands clearly enhanced. These features may be correlated with a preferential edge-on orientation of ZnPc on the substrate surface. The thermal treatment of the ZnPc film at 200 °C induces significant changes in the RAIRS spectrum. A prominent increase in the relative intensity of C–H out-of-plane mode at 719 cm^{-1} was observed and the in-plane modes are almost inactive. Metallic phthalocyanines form α-type polycrystalline films when evaporated onto substrates under 10^{-6} Torr vacuum at room temperature. Three polymorphs with different stacking sequences may be formed, α-I, α-II, and α-III [6]. The three main ZnPc stackings show that the ZnPc film may undergo phase transition from α-type to β-type polymorphs through metastable *x*-type in alcohol vapor [31]. Infrared data suggest a phase transition from α to β polymorphs through metastable *x*-form with a flat-on preferential orientation of macrocycle plane on the substrate surface after the annealing treatment. FTIR bands in the 700–800 cm^{-1} region, found mainly after annealing, indicate a β form of ZnPc [32].

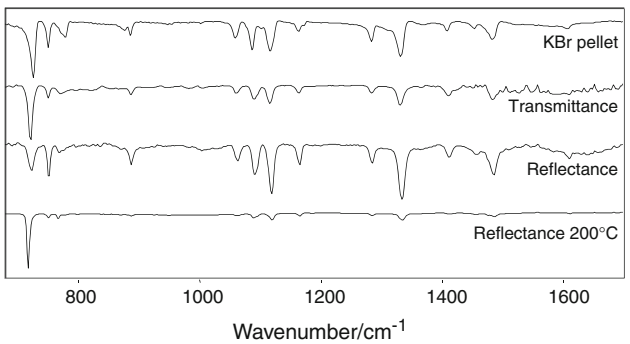

Fig. 2 FTIR spectra of ZnPc in KBr pellet; evaporated film over ZnSe (transmittance mode); and evaporated film over Au-coated glass substrate: as-deposited, and after annealing at 200 °C (reflectance mode)

The Raman spectra of the ZnPc evaporated films before and after annealing at 200 °C for 3 h are shown in Fig. 3. The bands observed in the spectra, their relative intensities (in parenthesis) and assignments are shown in Table 2. The most intense band before annealing was observed at 1509 cm^{-1}, relative to pyrrole stretch. After annealing, the most intense band shifted to 676 cm^{-1}, relative to the macrocycle breathing. The intensity of all bands increased after annealing, with the exception of the band at 1509 cm^{-1}. Note that some absorption may be observed for a film annealed at 200 °C at 514 nm, as observed in the inset of

Table 1 FTIR (transmission and RAIRS modes) characteristic vibrations of ZnPc KBr pellet and evaporated films, in cm^{-1}

KBr pellet	Transmission	RAIRS	RAIRS at 200 °C	Assignment
726 (100)	723 (100)	724 (46)	719 (100)	Out-of-plane C–H deformation
752 (47)	752 (22)	753 (62)	753 (6)	In-plane C–H deformation
777 (26)	774 (11)	773 (11)	769 (8)	Benzene breathing
888 (21)	888 (14)	889 (31)	888 (2)	
1060 (32)	1063 (14)	1064 (27)	1063 (3)	C–H bend
1088 (53)	1092 (24)	1093 (56)	1092 (7)	In-plane C–H bend
1118 (58)	1117 (32)	1120 (93)	1120 (11)	In-plane C–H bend
1165 (16)	1165 (11)	1166 (38)	1167 (5)	C–H bend
1291 (16)	1285 (14)	1286 (32)	1286 (4)	In-plane C–H bend
1332 (63)	1333 (35)	1335 (100)	1335 (12)	In-plane pyrrole stretch
1409 (16)	1413 (16)	1413 (22)	1414 (2)	Isoindole stretch
1460 (11)		1458 (15)	1457 (2)	Isoindole stretch
1483 (32)	1486 (24)	1485 (50)	1485 (6)	C=C benzene stretch
1584 (10)	1590 (14)			C=C benzene stretch
1606 (12)		1624 (16)	1612 (1)	C=C benzene stretch

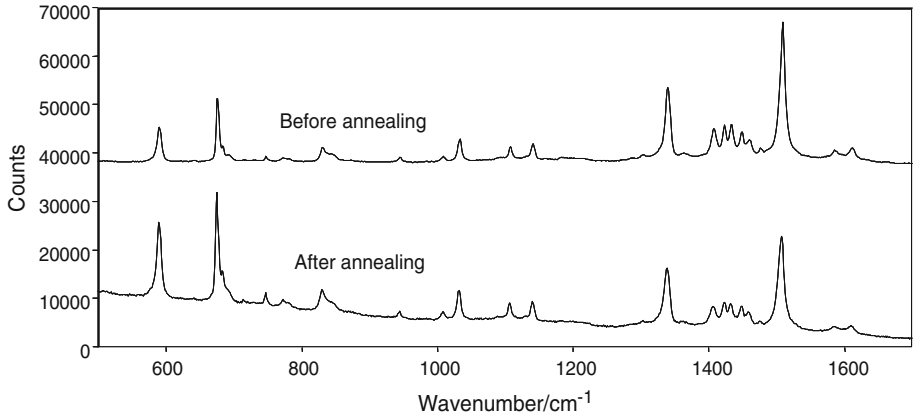

Fig. 3 Raman spectra of ZnPc evaporated film before and after annealing at 200 °C

Table 2 Raman characteristic molecular vibrations of ZnPc evaporated films (cm^{-1})

As-deposited sample	Annealed at 200 °C	Assignment
591 (25)	591 (69)	Benzene ring deformation
677 (46)	676 (100)	Macrocycle breathing
831 (11)	831 (20)	Out-of-plane ring deformation
1032 (3)	1032 (27)	C–H bend
1107 (11)	1106 (15)	C–H bend
1142 (13)	1141 (17)	Pyrrole ring deformation
1340 (54)	1338 (67)	Pyrrole stretch
1509 (100)	1507 (84)	Pyrrole stretch

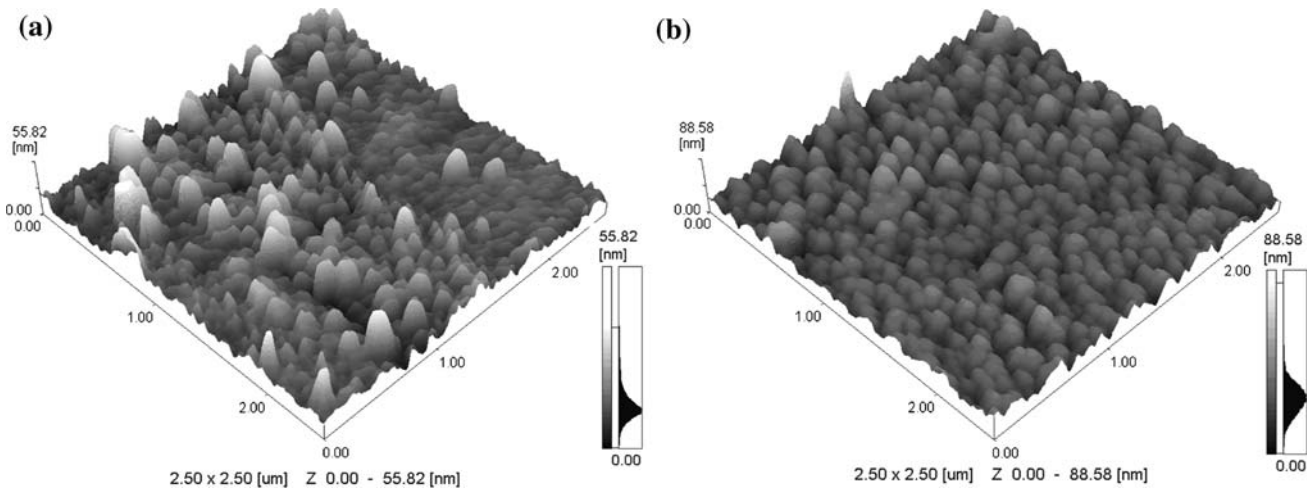

Fig. 4 AFM image of ZnPc evaporated film on mica before **a** and after **b** annealing at 200 °C

Fig. 1. This indicates that the laser is in resonance with the absorption spectra, inducing the increase in intensity observed after annealing [33]. The shift of the most intense band from 1509 to 676 cm^{-1} can be related with a change in the molecular structure of ZnPc [34].

The AFM images of a film before and after annealing are shown in Fig. 4. The image before annealing (Fig. 4a) shows a mixed morphology with only a small homogeneous region. After annealing, the film presented a more homogenous morphology with well-defined globular structures (Fig. 4b), which may be evidenced that most of the molecules are in flat-on orientation, according to the observed via FTIR analyses. The RMS roughness was estimated at 7.73 and 7.64 nm, before and after annealing, respectively. A similar morphology was obtained for ZnPc thin films by Sathyamoorthy et al. [35].

X-ray diffractograms for a ZnPc film evaporated over glass, as-deposited sample and after annealing at 200 °C, are displayed in Fig. 5. In the as-deposited films are observed predominant peaks at 6.88°, 9.66°, and 22.44°,

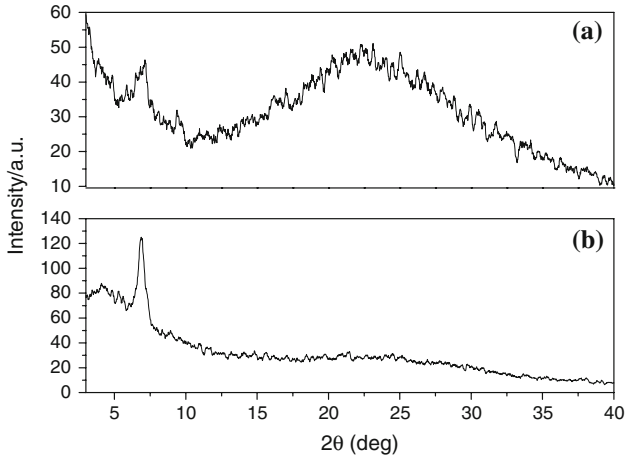

Fig. 5 XRD diffraction patterns of ZnPc films evaporated on glass before **a** and after **b** annealing at 200 °C

corresponding to an interplanar distance of 12.85, 9.16, and 3.96 Å, respectively. Note that a spacing of 3.96 Å corresponds to the very first layer of molecules lying parallel to the substrate surface [24]. After annealing at 200 °C for 3 h, the crystallinity of the films increased, as evidenced by the increase in peak intensity at 6.88°. Furthermore, the absence of the peak at 22.44°, suggests that those molecules from the first layer are no longer parallel to the substrate. Although X-ray diffraction data may be useful for evidencing a transition between α to β phases, such transition was not observed here, probably due to the very low thickness of the films [18, 32].

Conclusions

ZnPc was successfully synthesized and thin films were deposited by evaporation. UV–VIS spectroscopy showed a phase transition from α to β upon film annealing at 200 °C, which was also confirmed by FTIR measurements. The latter heating treatment also contributed to a better uniformity of the film, as evidenced by AFM analyses. FTIR analysis also suggested a polymorph phase transition through metastable *x*-form with the macrocycle in face-on orientation to the substrate surface. The presence of molecules lying parallel to the substrate was evidenced by X-ray diffraction analyses, however, an α to β phase transition was not observed, probably due to the low thickness of the films.

Acknowledgements We gratefully acknowledge Dr. Carlos José Leopoldo Constantino for the use of the Raman equipment and Dr. Eduardo Radovanovic for the AFM images. The authors also thank CAPES (PRODOC Program), CNPq, and FAPESP for the financial support.

References

1. Fernandes AN, Richardson TH (2008) J Mater Sci 43:1305. doi:10.1007/s10853-007-2184-7
2. Alarjah M, Paniwnyk L, Peterson IR, Lorimer JP, Walton DJ (2009) J Mater Sci 44:4246. doi:10.1007/s10853-009-3593-6
3. Alarjah M, Paniwnyk L, Peterson IR, Lorimer JP, Walton DJ (2009) J Mater Sci 44:5737. doi:10.1007/s10853-009-3803-2
4. Stevenson K, Miyashita N, Smieja J, Mazur U (2003) Ultramicroscopy 97:271
5. Ding H, Wang S, Xi S (1999) J Mol Struct 475:175
6. Guillaud G, Simon J, Germain JP (1998) Coord Chem Rev 178–180:1433
7. Crossley MS, Burn PL, Langford SJ, Prashar JK (1995) J Chem Soc Chem Commun 1921
8. Diaz-Garcia MA, Ledoux I, Duro JA, Tores T, Agullo-Lopez F, Zyss J (1994) J Phys Chem 98:8761
9. Eichhorn H, Wöhrle D, Presner D (1997) Liquid Cryst 22:643
10. Clavijo RE, Battisti D, Aroca R (1992) Langmuir 8:113
11. van Faassen E, Kerp H (2003) Sens Actuators B 88:329
12. Wróbel D, Boguta A (2002) J Photochem Photobiol A 150:67
13. Wöhrle D, Wendt A, Weitemeyer A, Stark J, Spileer W, Schneider G, Müller S, Michelsen U, Kliesch H, Heuermann A, Ardeschirpur A (1994) Russ Chem Bull 43:1953
14. Boyle RW, van Lier JE (1993) Synlett 351
15. Gaffo L, Brasil MJSP, Cerdeira F, Giles C, Moreira WC (2005) J Porphyr Phthalocyanines 9(2):89
16. Álvarez J, Souto J, Rodríguez-Mendez ML, de Saja JA (1998) Sens Actuators B 48:339
17. Valli L (2005) Adv Colloid Interface Sci 116:13
18. Heutz S, Bayliss SM, Middleton RL, Rumbles G, Jones TS (2000) J Phys Chem B 104:7124
19. Oriol JO, Schreiber F, Kruppa V, Dosh H, Garriga M, Alonso MI, Cerdeira F (2002) Adv Funct Mater 12:455
20. Schlettwein D, Hesse K, Tada H, Mashiko S, Storm U, Binder J (2000) Chem Mater 12:989
21. Jungyoon E, Kim S, Lim E, Lee K, Cha D, Friedman B (2003) Appl Surf Sci 205:274
22. Bayliss SM, Heutz S, Rumbles G, Jones TS (1999) Phys Chem Chem Phys 1:3673
23. Senthilarasu S, Sathyamoorthy R, Kulkarni SK (2005) Mater Sci Eng B 122:100
24. Senthilarasu S, Hahn YB, Lee SH (2007) J Appl Phys 102:043510
25. Kirin IS, Moskalev PN, Maskashev YA (1967) Russ J Inorg Chem 12:369
26. Gaffo L, Zucolotto V, Cordeiro MR, Moreira WC, Oliveira ON Jr, Cerdeira F, Brasil MJSP (2007) Thin Solid Films 515:7307
27. Ramamurthy V (1991) Photochemistry in Organized and Constrained Media. VHC, New York
28. Aroca R, Thedchanamoorthy A (1995) Chem Mater 7:69
29. Greenler RG (1996) J Chem Phys 44:310
30. Gobernado-Mitre MI, Aroca R (1995) Chem Mater 7:118
31. Iwatsu F, Kobayashi T, Uyeda N (1980) J Phys Chem 84:3223
32. El-Nahass MM, Zeyada HM, Aziz MS, El-Ghamaz NA (2004) Optical Material 27:491
33. Gaffo L, Constantino CJL, Moreira WC, Aroca RF, Oliveira ON Jr (2004) Spectrochim. Acta, Part A 60:321
34. Szybowicz M, Runka T, Drozdowski M, Baia W, Wojdyia M, Grodzicki A, Piszczek P, Bratkowski A (2007) J Mol Struct 830:14
35. Sathyamoorthy R, Senthilarasu S (2006) Sol Energy 80:201